Diffusion MRI of Parathyroid Adenomas using a Distortion Reduction Scheme

Hirotaka Yamamoto[1], Mami Iima[2], Yo Kishimoto[2], Ayami Kishimoto[2], Sho Koyasu[2], Akira Yamamoto[2], Yoshitaka Kawai[2], Akira Yoshizawa[2], and Koichi Omori[3]

[1]Tenri Hospital
[2]Kyoto University Graduate School of Medicine Faculty of Medicine
[3]Kyoto University

April 05, 2024

Abstract

Objectives: To evaluate whether readout-segmented echo-planar imaging (RS-EPI) diffusion-weighted imaging (DWI) can reduce image distortion and improve the lesion identification in parathyroid adenomas (PTAs) compared to single-shot EPI (SS-EPI) DWI, and to determine whether PTAs can be differentiated from other soft tissue structures of the head and neck region by using the apparent diffusion coefficient (ADC) value. Design: Retrospective study. Setting: Kyoto University Hospital. Participants: 24 patients who underwent a magnetic resonance imaging (MRI) scan for the preoperative diagnosis of PTAs from January 2012 to March 2020 were enrolled. Main outcome measures: MRI was performed with the acquisition of a 1.5T MR imaging system (Avanto or Trio, Siemens, Erlangen, Germany) or a 3T MR imaging system (Prisma or Skyra, Siemens). Image quality and distortion of PTAs on RS-EPI and SS-EPI was evaluated using a reported five point score, and the ADC values of PTAs, thyroid glands and cervical neck lymph nodes were compared. Results: RS-EPI provided significantly less distortion but did not improve the lesion identification compared to SS-EPI. On SS-EPI, the PTAs had significantly higher ADC values compared to the cervical lymph nodes. On RS-EPI, the PTAs had significantly higher ADC values compared to the thyroid glands and cervical lymph nodes. Conclusions: RS-EPI reduces the DWI distortion in PTAs. The ADC value obtained using RS-EPI enables the differentiation of PTAs from nearby structures, such as thyroid glands and cervical lymph nodes.

Article type: Original Article

Abstract

Objectives: To evaluate whether readout-segmented echo-planar imaging (RS-EPI) diffusion-weighted imaging (DWI) can reduce image distortion and improve the lesion identification in parathyroid adenomas (PTAs) compared to single-shot EPI (SS-EPI) DWI, and to determine whether PTAs can be differentiated from other soft tissue structures of the head and neck region by using the apparent diffusion coefficient (ADC) value.

Design : Retrospective study.

Setting : ⟨Blinded for review⟩

Participants : 24 patients who underwent a magnetic resonance imaging (MRI) scan for the preoperative diagnosis of PTAs from January 2012 to March 2020 were enrolled.

Main outcome measures : MRI was performed with the acquisition of a 1.5T MR imaging system (Avanto or Trio, Siemens, Erlangen, Germany) or a 3T MR imaging system (Prisma or Skyra, Siemens).

Image quality and distortion of PTAs on RS-EPI and SS-EPI was evaluated using a reported five point score, and the ADC values of PTAs, thyroid glands and cervical neck lymph nodes were compared.

Results: RS-EPI provided significantly less distortion but did not improve the lesion identification compared to SS-EPI. On SS-EPI, the PTAs had significantly higher ADC values compared to the cervical lymph nodes. On RS-EPI, the PTAs had significantly higher ADC values compared to the thyroid glands and cervical lymph nodes.

Conclusions: RS-EPI reduces the DWI distortion in PTAs. The ADC value obtained using RS-EPI enables the differentiation of PTAs from nearby structures, such as thyroid glands and cervical lymph nodes.

Keywords: parathyroid adenoma, readout-segmented echo-planar imaging, diffusion-weighted-MRI, apparent diffusion coefficient

Wordcount main article: 2278

Key points:

- The Kappa values between the two readers revealed substantial-to-perfect agreement.
- RS-EPI provided significantly less distortion compared to SS-EPI, however the structure identification scores were not significantly different from SS-EPI.
- The PTAs exhibited relatively high signal intensity on DW-MRI with either SS-EPI or RS-EPI.
- On SS-EPI, the PTAs had significantly higher ADC values compared to the cervical lymph nodes.
- On RS-EPI, the PTAs had significantly higher ADC values compared to the thyroid glands and cervical lymph nodes.

Introduction

Primary hyperparathyroidism (PHPT) is a clinical condition characterized by elevated serum parathyroid hormone (PTH), followed by increased serum calcium (Ca). Patients with PHPT frequently manifest symptoms such as hypercalcemia, anorexia, nausea, and nephrocalcinosis. The treatment for PHPT used to be a total parathyroidectomy, but PHPT is usually caused by a single parathyroid adenoma (PTA)(1, 2), and selective parathyroidectomy has been recently preferred for the treatment of single adenomas as a less invasive option(3, 4). For a successful selective parathyroidectomy, accurate imaging techniques are required for the preoperative localization of PTAs. Ultrasonography and technetium 99mTc-sestamibi scintigraphy have often been accepted as first-line imaging to localize PTAs. When first-line imaging fails to localize the parathyroid lesion, or PHPT is recurrent or persistent after surgery, computed tomography (CT) and magnetic resonance imaging (MRI) are considered as second-line imaging techniques (1, 5). Recently, the multiphasic CT (4D CT) has made it possible to identify PTAs through their hypervascular perfusion pattern compared with lymph nodes and thyroid gland(5), however CT has the disadvantage of ionizing radiation.

MRI has the advantage of lack of ionizing radiation, and with the introduction of high field magnetic systems, the use of MRI for the localization of parathyroid adenomas has been re-assessed as a supplemental imaging modality. The sensitivity of 1.5T MRI for the detection of PTAs was reported to be 43%–71%(6-8), but since 3T scanners were introduced into clinical practice in the early 2000s, the higher signal-to-noise and contrast-to-noise ratios have improved the sensitivity of MRI to 97.8%.(1) However, some limitations remain because the MR appearance of PTAs overlaps considerably with those of cervical lymph nodes and an ectopic thyroid gland, which leads to difficulties in distinguishing PTAs from other structures in the neck.

The measurement of the apparent diffusion coefficient (ADC) value in diffusion-weighted imaging (DWI) has been reported to be helpful in distinguishing parathyroid tissues from other soft-tissue structures of the head and neck region.(9) Single-shot echo-planar imaging (SS-EPI) has been the most widely used DWI sequence, but SS-EPI suffers from susceptibility artifacts which manifest as geometric distortion and image blurring,(10) and the detection of PTAs by DWI thus remains challenging. To overcome this weakness, readout-segmented echo-planar imaging (RS-EPI) was developed; with this imaging modality, there is a substantial reduction in the distortion and blurring caused by T2* decay during the readout(11, 12). RS-

EPI is expected to improve the diagnostic accuracy of detecting PTAs on DWI as it provides less distortion, and its advantages are reported in some organs including the head and neck(13-15).

However, to our knowledge, there is no literature focusing on the usefulness of RS-EPI for the localization and distinction of PTAs. We conducted the present retrospective study to determine whether RS-EPI can reduce image distortion and improve the lesion identification in PTAs compared to SS-EPI, and to determine whether PTAs can be differentiated from other soft-tissue structures of the head and neck region by using the ADC value.

Materials and Methods

MRI examination

The MRI examinations in this study were performed with a 1.5T MR imaging system (Avanto or Trio, Siemens, Erlangen, Germany) or a 3T MR imaging system (Prisma or Skyra, Siemens). The parameters for the DWI sequences are summarized in **Table 1** .

Setting and Participants

This study was approved by the institutional review board of 〈Blinded for review〉 . A total of 34 patients with PTA who underwent an MRI examination for the preoperative diagnosis of PTA at 〈Blinded for review〉 during the period from January 2012 to March 2020 were examined. SS-EPI at 1.5T was performed in eight patients during the period Jan. 2012 to Nov. 2017, and RS-EPI at 3.0T was performed in 26 patients during the period July 2014 to March 2020. All patients underwent a parathyroidectomy, and the resected specimens were histologically evaluated. Of the 34 patients, 10 patients were excluded from this study for the following reasons: the lesion was not detectable on MRI (n=3), DWI data were obtained using a different protocol (n=5), and the presence of severe motion or susceptibility artifacts (n=2). The remaining 24 patients were enrolled. Their clinical information including the results of imaging examinations was retrospectively reviewed.

Analysis of image quality and distortion

Board-certified radiologists A and B independently evaluated the image quality and the distortion of parathyroid lesions on DWI. They had access to other MR images (T2- or T1-weighted images or STIR image) for a reference. They were informed that the DWIs were acquired for the preoperative evaluation of PTA, and they were unaware of any other radiologic information. Structural identification and geometric distortion were evaluated using a reported five-point scale (Table 2).(13)

Measurements of ADC values

ADC measurements of the lesions were performed on the ADC map that contained the largest lesion cross-section, using circular regions-of-interest (ROIs) with a mean area of 10 mm^2. Each ROI was carefully drawn within the solid part of the lesion to exclude artifacts and areas of cyst and/or necrosis. The ADC values of each patient's cervical lymph nodes and thyroid glands were also measured.

The DWI statistical analysis

The inter-observer variability between the wo radiologists was evaluated using inter-rater agreement (Kappa coefficient). As described,(16) the results were interpreted as follows: values [?]0 indicate no agreement; 0.01–0.20 indicate none to slight agreement, 0.21–0.40 = fair agreement, 0.41–0.60 = moderate, 0.61–0.80 = substantial, and 0.81–1.00 = almost perfect agreement.(17) The ADC values of the parathyroid lesions, thyroid glands, and cervical lymph nodes were analyzed using the Friedman test with Bonferroni correction, and the scores of structure identification and geometric distortion on SS-EPI and RS-EPI were compared using the median test. In both tests, p-values <0.05 were accepted as significant. All statistical analyses were performed with EZR (Saitama Medical Center, Jichi Medical University), which is a graphical user interface for R (The R Foundation for Statistical Computing, Vienna, Austria, ver. 2.13.0).(18)

Results

Patients and lesions

The patient and lesion characteristics are summarized in **Table 3** . The SS-EPI group was two males and six females (mean age 64 years, range 48–76 years), and the RS-EPI group was six males and 10 females (mean age 55.6 years, range 25–80 years). All lesions were pathologically diagnosed as parathyroid adenomas, and there were no significant differences in patient or lesion characteristics between the two groups.

Assessments of structure identification and distortion

The Kappa values between the two readers revealed substantial-to-perfect agreement (structure identification provided by SS-EPI: 0.73, distortion by SS-EPI: 1, identification by RS-EPI: 0.75, distortion by RS-EPI: 0.82). The mean scores of structure identification and geometric distortion for SS-EPI and RS-EPI by the two readers are shown in**Table 4** . The distortion scores for RS-EPI were significantly higher than those for SS-EPI (all p-values were <0.05), indicating lower distortion, and the image quality provided by RS-EPI was better than that obtained with SS-EPI. However, the results of the median test of the structure identification scores were not significantly different between SS-EPI and RS-EPI.

Representative cases

Representative cases of SS-EPI and RS-EPI are shown in **Figures 1** and **2** . A 67-year-old female was diagnosed as having a PTA of the right inferior gland and presented high intensity mass on STIR; however, there was considerable distortion on SS-EPI (Fig. 1). In contrast, in the case of a 72-year-old female with a PTA at the left inferior gland with DWI using RS-EPI, the lesion was identified with less distortion (Fig. 2).

Discrimination of PTAs from the thyroid gland and cervical lymph nodes using ADCs

The PTAs exhibited relatively high signal intensity on DW-MRI with either SS-EPI or RS-EPI, with high ADC values. On SS-EPI, the average ADC values of the PTAs, thyroid glands, and cervical lymph nodes were 1.44, 1.07, and 0.80 $\times$ 10^{-3} mm^2/s, respectively, and a significant difference between the PTAs and lymph nodes was observed. Moreover, the average ADC values of the PTAs, thyroid glands, and cervical lymph nodes were 1.67, 1.46, and 0.95 x 10^{-3} mm^2/s on RS-EPI, and the PTAs exhibited significantly higher ADC values compared to those of the thyroid glands and lymph nodes (Fig. 3).

Discussion

We evaluated the clinical utility of DWI for the pre-operative localization of PTAs. While the PTAs were faintly identified with intense distortion on SS-EPI, they were fairly identified with moderate distortion on RS-EPI. The inter-rater reliability was substantial or perfect, and the validity of DW-MRI for the localization of PTAs was demonstrated. In addition, the PTAs could be discriminated from cervical lymph nodes and thyroid glands by measuring the ADC values, and thus RS-EPI is expected to become the optimal diagnostic modality for the localization of PTAs.

With the introduction of 3T MRI, improved diagnostic performance for the detection of PTAs has been reported in relation to the higher spatial resolution and contrast-to-noise ratio.(1) PTAs are usually T2 hyperintense, and fat suppression is effective to achieve an accurate depiction.(1) However, fat suppression is not easy to use in the neck region, especially in the mediastinum, because of the magnetic field inhomogeneities due to the proximity of lungs and upper airways. It thus remains challenging to obtain good images of PTAs with MRI, and there is currently no consensus on the optimal MRI protocol for the evaluation of PTAs.

The diagnostic value of 4D MRI and of the IDEAL sequence for the detection of PTAs has been reported.(19, 20) Although the use of these imaging techniques improved the diagnostic sensitivity for the detection of PTAs, false-positive diagnoses are occasionally attributed to cervical lymph nodes or adjacent/ectopic thyroid tissues. To distinguish PTAs from lymph nodes and thyroid tissues, Yildiz et al. used conventional DWI provided by a 1.5T system, and they reported higher ADC values in parathyroid lesions compared to lymph nodes and thyroid tissues; however, the statistical significance of these differences was not reported.(9)

Although SS-EPI is a well-established conventional method for the acquisition of DWI data with short scan times, it suffers from geometric distortion, signal dropout, and image blurring. Alternatively, RS-EPI is a multi-shot sequence that reduces susceptibility artifact and blurring arising from T2* decay, and thus lower distortion can be achieved.(21) The clinical utility of RS-EPI has been well documented in some regions, including the head and neck.(13) In our present case series, the acquisition parameters were quite different between RS-EPI and SS-EPI, because they were independently set to optimize their image quality within clinically acceptable acquisition times (2–3 min). Since a sufficient signal-to-noise ratio (SNR) was not expected for SS-EPI, the number of excitations were increased to four. A sufficient SNR was expected for RS-EPI, so we increased the number of readout segments to five, to reduce the distortion. The results demonstrated that the PTAs were well identified with less distortion by RS-EPI compared to SS-EPI, and the conclusions of the two independent readers showed a good correlation.

RS-EPI is thought to be a useful and reliable imaging technique for the evaluation of PTAs. However, we observed herein that even with RS-EPI, some PTAs were poorly identified with intense distortion, which might mask the improvement in the lesion identification score. The distortion might come from (1) the relatively large field of view (FOV) needed to obtain whole neck images, (2) susceptibility artifact that remained even with RS-EPI, and/or (3) motion artifact from respiration. In addition, it is not still easy to obtain good-quality DW images at the upper mediastinum due to the complex stricture facing the air, and the establishment of a feasible imaging protocol of the cervical region to the upper mediastinum using DW-MRI is expected.

In this study, we used ADC values for discriminating the PTAs and other cervical organs, and the PTAs were well distinguished from the thyroid glands and cervical lymph nodes. Cervical lymph nodes exhibit low ADC values,(22) and benign neck pathologies including adenomas are reported to show relative high ADC values,(23, 24) which is consistent with our present observations. Higher ADC values were observed on RS-EPI compared to SS-EPI in our case series. Differences in ADC values between RS-EPI and SS-EPI are still controversial. Although higher ADC values on RS-EPI have been reported in the human mammary gland and in a phantom study,(21, 25) Koyasu et al. reported no significant differences in the ADCs of salivary gland lesions.(13) In our present cases, the accurate evaluation of lesions due to less distortion on 3T RS-EPI may have contributed to the precise selection of the area, while more distorted lesions on 1.5T SS-EPI might have been contaminated by surrounding fat tissue and consequently resulted in a decreased ADC, which we observed particularly in the thyroid glands. Adding DWI using RS-EPI to common sequences such as STIR and T2WI could thus be beneficial for the pre-operative evaluation of PTAs.

This is the first study to investigate the clinical utility of RS-EPI in the pre-operative localization of PTAs, to our knowledge. One of the limitations of our study was its retrospective design. In addition, the acquisition protocols for SS-EPI and RS-EPI were independently set to maximize their own features (rather than a comparison of the two protocols), which resulted in different acquisition schemes. The sample size was small, and there would be a selection bias because selected patients with surgically confirmed pathologies were included. Further prospective studies with larger sample sizes are warranted to clarify the diagnostic utility, indications, and limitations of RS-EPI for the localization of PTAs.

Conclusion

Our study demonstrated that RS-EPI produces images with less DWI distortion than SS-EPI, which may provide clinical advantages in the localization of PTA. And PTAs have higher diffusion properties compared with thyroid glands, and cervical lymph nodes using RS-EPI. This feature enables us to the differentiation of PTAs from nearby structures on MRI.

References

1. Argiro R, Diacinti D, Sacconi B, Iannarelli A, Cipriani C, Pisani D, et al. Diagnostic accuracy of 3T magnetic resonance imaging in the preoperative localisation of parathyroid adenomas: comparison with ultrasound and 99mTc-sestamibi scans. Eur Radiol. 2018;28(11):4900-8.

2. Bartsch D, Nies C, Hasse C, Willuhn J, Rothmund M. Clinical and surgical aspects of double adenoma in patients with primary hyperparathyroidism. Br J Surg. 1995;82(7):926-9.

3. Smit PC, Borel Rinkes IH, van Dalen A, van Vroonhoven TJ. Direct, minimally invasive adenomectomy for primary hyperparathyroidism: An alternative to conventional neck exploration? Ann Surg. 2000;231(4):559-65.

4. Sackett WR, Barraclough B, Reeve TS, Delbridge LW. Worldwide trends in the surgical treatment of primary hyperparathyroidism in the era of minimally invasive parathyroidectomy. Arch Surg. 2002;137(9):1055-9.

5. Nael K, Hur J, Bauer A, Khan R, Sepahdari A, Inampudi R, et al. Dynamic 4D MRI for Characterization of Parathyroid Adenomas: Multiparametric Analysis. AJNR Am J Neuroradiol. 2015;36(11):2147-52.

6. Kunstman JW, Kirsch JD, Mahajan A, Udelsman R. Clinical review: Parathyroid localization and implications for clinical management. J Clin Endocrinol Metab. 2013;98(3):902-12.

7. Ruf J, Lopez Hanninen E, Steinmuller T, Rohlfing T, Bertram H, Gutberlet M, et al. Preoperative localization of parathyroid glands. Use of MRI, scintigraphy, and image fusion. Nuklearmedizin. 2004;43(3):85-90.

8. Wakamatsu H, Noguchi S, Yamashita H, Tamura S, Jinnouchi S, Nagamachi S, et al. Parathyroid scintigraphy with 99mTc-MIBI and 123I subtraction: a comparison with magnetic resonance imaging and ultrasonography. Nucl Med Commun. 2003;24(7):755-62.

9. Yildiz S, Aralasmak A, Yetis H, Kilicarslan R, Sharifov R, Alkan A, et al. MRI findings and utility of DWI in the evaluation of solid parathyroid lesions. Radiol Med. 2019;124(5):360-7.

10. Holdsworth SJ, Yeom K, Skare S, Gentles AJ, Barnes PD, Bammer R. Clinical application of readout-segmented- echo-planar imaging for diffusion-weighted imaging in pediatric brain. AJNR Am J Neuroradiol. 2011;32(7):1274-9.

11. Porter DA, Heidemann RM. High resolution diffusion-weighted imaging using readout-segmented echo-planar imaging, parallel imaging and a two-dimensional navigator-based reacquisition. Magn Reson Med. 2009;62(2):468-75.

12. Porter DA, Calamante F, Gadian DG, Connelly A. The effect of residual Nyquist ghost in quantitative echo-planar diffusion imaging. Magn Reson Med. 1999;42(2):385-92.

13. Koyasu S, Iima M, Umeoka S, Morisawa N, Porter DA, Ito J, et al. The clinical utility of reduced-distortion readout-segmented echo-planar imaging in the head and neck region: initial experience. Eur Radiol. 2014;24(12):3088-96.

14. Klingebiel M, Ullrich T, Quentin M, Bonekamp D, Aissa J, Mally D, et al. Advanced diffusion weighted imaging of the prostate: Comparison of readout-segmented multi-shot, parallel-transmit and single-shot echo-planar imaging. Eur J Radiol. 2020;130:109161.

15. Kishimoto AO, Kataoka M, Iima M, Honda M, Miyake KK, Ohashi A, et al. Evaluation of Malignant Breast Lesions Using High-resolution Readout-segmented Diffusion-weighted Echo-planar Imaging: Comparison with Pathology. Magn Reson Med Sci. 2020.

16. Landis JR, Koch GG. An application of hierarchical kappa-type statistics in the assessment of majority agreement among multiple observers. Biometrics. 1977;33(2):363-74.

17. McHugh ML. Interrater reliability: the kappa statistic. Biochem Med (Zagreb). 2012;22(3):276-82.

18. Kanda Y. Investigation of the freely available easy-to-use software 'EZR' for medical statistics. Bone Marrow Transplant. 2013;48(3):452-8.

19. Memeh KO, Palacios JE, Khan R, Guerrero MA. PRE-OPERATIVE LOCALIZATION OF PARATHYROID ADENOMA: PERFORMANCE OF 4D MRI PARATHYROID PROTOCOL. Endocr Pract. 2019;25(4):361-5.

20. Ozturk M, Polat AV, Celenk C, Elmali M, Kir S, Polat C. The diagnostic value of 4D MRI at 3T for the localization of parathyroid adenomas. Eur J Radiol. 2019;112:207-13.

21. Kanao S, Kataoka M, Iima M, Ohno A, Sakaguchi R, Ohashi A, et al. High-resolution diffusion-weighted MRI of the breast using readout-segmented EPI and single-shot EPI. Imaging in Medicine. 2017;9:185-90.

22. Moreau B, Iannessi A, Hoog C, Beaumont H. How reliable are ADC measurements? A phantom and clinical study of cervical lymph nodes. Eur Radiol. 2018;28(8):3362-71.

23. Kanmaz L, Karavas E. The Role of Diffusion-Weighted Magnetic Resonance Imaging in the Differentiation of Head and Neck Masses. J Clin Med. 2018;7(6).

24. Srinivasan A, Dvorak R, Perni K, Rohrer S, Mukherji SK. Differentiation of benign and malignant pathology in the head and neck using 3T apparent diffusion coefficient values: early experience. AJNR Am J Neuroradiol. 2008;29(1):40-4.

25. Ihalainen T, Kuusela L, Soikkeli M, Lantto E, Ovissi A, Sipila O. A body-sized phantom for evaluation of diffusion-weighted MRI data using conventional, readout-segmented, and zoomed echo-planar sequences. Acta Radiol. 2016;57(8):947-54.

Table 1. Parameters for DWI

	SS-EPI (1.5T)	**RS-EPI (3T)** [++]
b-value, sec/mm^2	0, 1000	0, 1000
FOV	180*180	211*220
Matrix	192*192[+]	142*148
TR	5900	4100
TE	81	54
Slice thickness, mm	4	3
Fat suppression	STIR	SPAIR
Averages	4	1
Acquisition time, min:sec	2	2:15

[+]The matrix for SS-EPI is interpolated.[++]Five readout segments are used. FOV: field of view.

Table 2. Scales for structure identification and geometric distortion on DWI (modified from ref. 13)

Scales for structural identification

4	Excellent: Perfectly demarcated contour and very good contrast with surrounding structur
3	Good: Almost good contour, but partially (<50%) mixed with the background
2	Fair: Organ/node can be discriminated from surrounding structures, while more than half
1	Faint: Structures of organ/nodes are ill-defined, but can be identified by faint contrast wit
0	Unidentifiable: Cannot identify any structures
Scales for geometric distortion	Scales for geometric distortion
4	High geometric accuracy and almost no distortion
3	Faint distortion: Organ/node slightly tilts, but its convexity is almost the same as that of
2	Moderate distortion: Convexity is less pronounced or lost compared to that of a T2-weight
1	Intense distortion: Convexity is opposite compared to that of a T2-weighted TSE image, o
0	Impossible to evaluate, or unidentifiable

Table 3. Patient and lesion characteristics

No. of patients
Sex
Male
Female
Mean age (range), years
Location of lesion
Right superior
Right inferior
Left superior
Left inferior
Size of lesion, mm
Comparisons between the SS-EPI and RS-EPI were performed by Chi-square test for sex, and by median test for age and si

Table 4. Evaluation of structural identification and geometric distortion using a five-point scale

	Reader 1
	SS-EPI
Identification of structure	1.63±0.92
Geometric distortion	1.38±0.92
Data are mean ± SD. Comparisons between SS-EPI and RS-EPI were performed by median test. *p<0.05.	Data are mea

Figure Legends

fig. 1. Representative SS-EPI images of a 67-year-old female with primary hyperparathyroidism. **A:** STIR: A high-intensity mass on STIR was detected behind the right lobe of the thyroid gland.**B:** DWI with SS-EPI: A faint high-intensity lesion on DWI was detected in the corresponding location on STIR. The image was scored to be impossible to evaluate by two readers. **C:** ADC map: A high value was detected on the ADC map. The lesion was diagnosed as a PTA of the right superior gland. A 21 x 16 x 17 mm PTA was confirmed at surgery

Fig. 2. Representative RS-EPI images of a 72-year-old female with primary hyperparathyroidism. **A:** STIR: A high-intensity mass on STIR was detected behind the left lobe of the thyroid gland.**B:** DWI with RS-EPI: A high-intensity lesion on DWI was detected in the corresponding location on STIR. The lesion was evaluated as showing almost no or faint distortion. **C:** ADC map: A high value was detected on the ADC map. The lesion was diagnosed as a PTA of the left inferior gland. A 28 x 22 x 5 mm PTA was confirmed at surgery

Fig. 3. The ADC values of the parathyroid lesions, thyroid glands, and cervical lymph nodes. *Left:* SS-EPI. *Right:*RS-EPI. *p<0.05

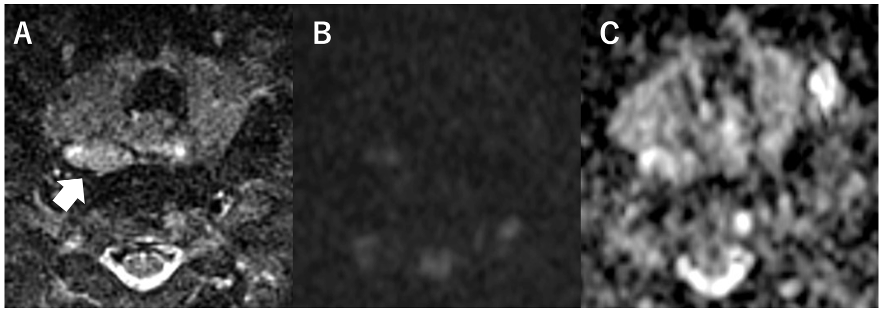
A
B
C

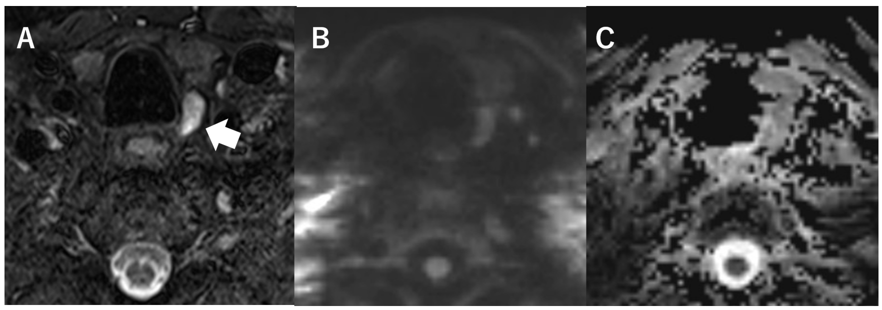
A
B
C

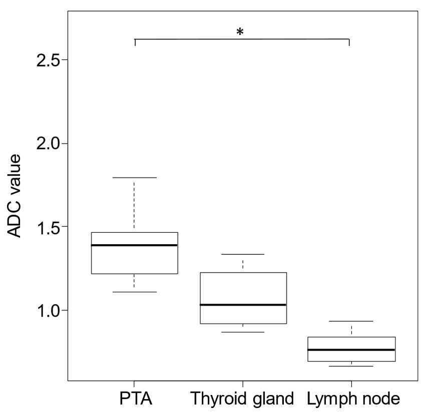
*
ADC value
2.5
2.0
1.5
1.0
PTA
Thyroid gland
Lymph node

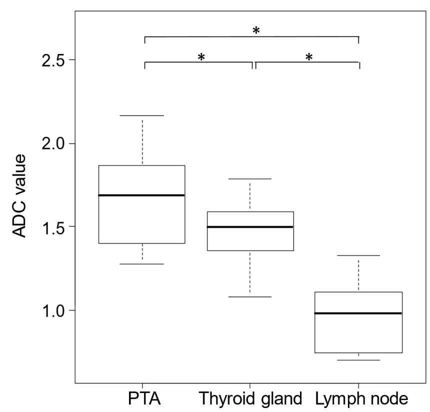
*
*
*
ADC value
2.5
2.0
1.5
1.0
PTA
Thyroid gland
Lymph node